coatings

MDPI

Article

Thermal Tunable Tribological Behavior of Shape Memory Biphenyl Epoxy Resin

Jing Yang [1,2], Pengrui Cao [1,3], Ketian Gao [1,4], Chang Ding [1,4], Shoubing Chen [1,3], Xinrui Zhang [1,3], Tingmei Wang [1,3,*], Qihua Wang [1,3,*] and Yaoming Zhang [1,3,*]

1 Key Laboratory of Science and Technology on Wear and Protection of Materials, Lanzhou Institute of Chemical Physic, Lanzhou 730000, China
2 Yantai Zhongke Research Institute of Advanced Materials and Green Chemical Engineering, Yantai 264006, China
3 Center of Materials Science and Optoelectronics Engineering, University of Chinese Academy of Sciences, Beijing 100049, China
4 College of Petrochemical Technology, Lanzhou University of Technology, Lanzhou 730050, China
* Correspondence: tmwang@licp.cas.cn (T.W.); wangqh@licp.cas.cn (Q.W.); yaomingzhang@licp.cas.cn (Y.Z.)

Abstract: Although polymer-based self-lubricating materials have rapidly developed recently, intelligent lubricating materials with self-adaptable lubrication with external conditions changing are highly demanded, especially for harsh conditions. Herein, a shape memory epoxy resin based on the biphenyl units (BPEP) with tunable tribological behavior was systematically studied. X-ray diffraction (XRD), field emission scanning electron microscope (SEM), laser confocal three-dimensional profiler, and optical microscope were applied to analyze the friction and wear mechanism. Due to the presence of the specific biphenyl structural units, which could be performed a switching phase between crystalline and amorphous, that allows the self-assembly of the polymer chain under π–π interaction. As a result, the improving mechanical properties enable the BPEP to perform outstanding self-lubricating in a wide temperature range, and the friction coefficient (COF) can be tuned in a wide range of 0.10~0.175 by adjusting the temperature. The shape memory effect of the polymer refers to modulus changing and heat conversion during the shape morphing, and a thermal tunable tribological was observed based on the physicochemical properties varying of polymer with temperature changing. The shape memory effect of BPEPs drives the wear self-compensation so that a low wear rate (6.94×10^{-5} mm^3 N^{-1} m^{-1}) at 110 °C was obtained. The superb lubricating properties of this BPEP could broaden the application scope of shape memory polymers in the field of intelligent lubricating materials, and it is expected to guide future studies on the thermal regulating of tribological behavior.

Keywords: self-lubrication; shape memory epoxy resin; friction coefficient; tunable tribological behavior

check for updates

Citation: Yang, J.; Cao, P.; Gao, K.; Ding, C.; Chen, S.; Zhang, X.; Wang, T.; Wang, Q.; Zhang, Y. Thermal Tunable Tribological Behavior of Shape Memory Biphenyl Epoxy Resin. *Coatings* **2023**, *13*, 166. https://doi.org/10.3390/coatings13010166

Academic Editor: Alexander D. Modestov

Received: 17 December 2022
Revised: 7 January 2023
Accepted: 10 January 2023
Published: 12 January 2023

Copyright: © 2023 by the authors. Licensee MDPI, Basel, Switzerland. This article is an open access article distributed under the terms and conditions of the Creative Commons Attribution (CC BY) license (https://creativecommons.org/licenses/by/4.0/).

1. Introduction

As well known, lubrication provides the most effective way of anti-friction and anti-wear to prolong the service life of the machine. However, it is unattainable to maintain the demanded lubricating for the traditional lubrication materials when it serves in a variable condition that the intelligent lubrication materials (ILM) came into being. ILM, which perform perceives external stimuli and thus produces controllable and adjustable lubricating behaviors, is highly demanded in a broad scope of the tribological field [1]. Currently, the concept of ILM involves storing liquid lubricants [2], self-healing [3], self-cleaning [4,5], self-adaptive [6], and self-reporting [7] functions, that these materials could either diagnose the wear loss or response to the friction with a performance tuning that avoiding a replacement of the parts. Generally, combining different lubricants with specific structures could perform tunable tribological with the external environment changing; its lubrication performance strongly depends on the dispersion uniformity and lubricant

release [8]. Wang et al. reported that the intelligent lubricating material impregnated with different lubricants into porous polyimide can realize the release and recovery of lubricants through thermal, mechanical stimulation and capillarity [9,10]; this stimuli-responsive behavior realizes sustainable, intelligent lubrication. Although stimuli-responsive polymer materials, which are readily offering physicochemical properties varying in response to the stimuli, can be considered promising candidates for ILM, there are rare reports on the ILM based on stimuli-responsive materials because realizing the matching between responsive and desired tribological behavior remains a challenge. At present, the research based on stimuli-responsive polymer ILM mainly focuses on polymer brushes [11,12], microgels, biomimetic lubricating materials based on polymer [13], hydrogels, or ionic gels [14–16]. However, the feature of the soft materials constrained the practical application, such as poor mechanical properties, complex structures, and additional lubricants are required in some cases.

Shape memory polymer (SMP), which store and release energy under external stimuli (such as light [17], electricity [18], heat [19], magnetism, pH, etc.) accompany the morphing, and mechanical properties change during the shape memory cycle, is a promising ILM [20]. First, the mechanical properties of the SMP are determined by the temperature, and the modulus gradually decreases with the increase in temperature. Wang et al. [21] first explored the tribological properties dependence of SMP on temperature. The friction coefficient (COF) can be adjusted in a wide range of 0.14~1.09 by adjusting the temperature (from room temperature to above the glass transition temperature (T_g)). This significant change is mainly due to the change in the recovery stress caused by the shape memory effect. Second, the shape varying offers a possibility to tune the friction surface roughness to control the lubrication performance [22,23]. Broer et al. [24] reported that switching the wavelength of light on the surface could realize the reversible morphology tuning of the coating that achieves dynamic controlling tribological properties. This shows that the change of morphology can not only realize the adjustable COF (dry friction state) between 0.2 and 0.6 but also dynamically reduce the contact area of the friction interface, thereby reducing the friction forces. On the other hand, friction heat accumulation usually reduces the mechanical properties of the material, especially for polymer at the friction interface, and then leads to lubrication decay [25]. The morphing of SMP is always accompanied by energy conversion, mostly thermal energy; therefore, the application of the shape memory effect in regulating friction heat effectively provides a new strategy for ILM.

Previously, we reported the preparation of shape memory diphenyl epoxy resin (BPEPs) containing both strength and toughness by using aromatic amine with the high active functional group and the rigid backbone of benzene ring as a curing agent and diglycidyl ether containing biphenyl unit as an epoxy monomer by photocuring assisted amine thermal curing [26]. The crosslinking density of the polymer network can be easily tuned by simply adjusting the feed ratio of the epoxy monomer and the curing agent, which allows BPEP to exhibit a thermal tunable shape memory effect. In addition, the special post-heating treatment induced self-assembly of the biphenyl unit due to the π–π interaction, which not only improved the crosslink density of the network but also provided reconfigurable performance. It is reported that the unique layered structure formed by the π–π interaction can also improve the mechanical properties and thermal conductivity of the polymer [27,28]; this may help to improve its tribological properties.

In this study, the thermal tunable tribological behavior of shape memory biphenyl epoxy was investigated. The friction at varying temperatures from room temperature to above transition temperature was comparably studied, BPEPs performed outstanding self-lubricating in a wide temperature range, and it presented the thermal tunable tribological behavior from room temperature to above the glass transition temperature (T_g). Furthermore, friction induced the self-assembly of biphenyl structural units at high temperatures due to the π–π interaction can enhance its mechanical properties and coefficient of thermal conductivity and reduce the wear rate. This work explored a thermal-regulated

lubricating material based on shape memory polymers and is expected to pave the way for the development of new intelligent lubricating materials.

2. Materials and Methods

2.1. Materials

To prepare the shape memory epoxy resin with high toughness, the monomer containing biphenyl mesogen of diglycidyl ether of biphenyl (DGEBP) and the aromatic curing agent of M-xylylenediamine (M-XDA) were used for the synthesis. 4, 4′-Dihydroxybiphenyl and Epichlorohydrin were used to synthesize the epoxy monomer of DGEBP, which were purchased from Energy Chemical, Shanghai, China, and Chengdu Cologne Chemicals Co., Ltd., Chengdu, China, respectively. M-XDA was purchased from J&K, Beijing, China as a curing agent. N, N-dimethylacetamide (DMAC), isopropanol, toluene, ethanol, and other solvents were purchased from Li and Long Bo Hua Pharmaceutical chemical Co., Ltd, Tianjin, China. Irgacure 250 (I-250) as a cationic photoinitiator to initiate the reaction of epoxy with an amine under UV light, was purchased from Guangzhou Lihou Trading Co., Ltd., Guangzhou, China.

2.2. Preparation of Biphenyl Epoxy Resin Films (BPEPs)

The synthetic scheme of biphenyl epoxy resin (BPEPs) is shown in Scheme 1. Firstly, the epoxy monomer of diglycidyl ether of biphenyl (DGEBP) was synthesized through the substitution reaction between 4, 4′-dihydroxybiphenyl and epichlorohydrin under the catalysis of NaOH [29]. Then, biphenyl containing shape memory epoxy resin (BPEPs) with different crosslinking densities was prepared according to our previous report by a photocuring-assisted amine thermal curing with M-XDA as the curing agent, the resin was first placed under a high-pressure mercury lamp for 15 min and then transferred to vacuum oven at 55 °C for 48 h for drying [26]. The crosslinking density of BPEPs was controlled by adjusting the molar ratio of epoxy/amino groups, 1: 0.5, 1: 0.68, and 1: 0.86 were adopted, respectively, to prepare BPEP1, BPEP2, and BPEP3. The film with a thickness of about 0.5 mm was prepared by casting.

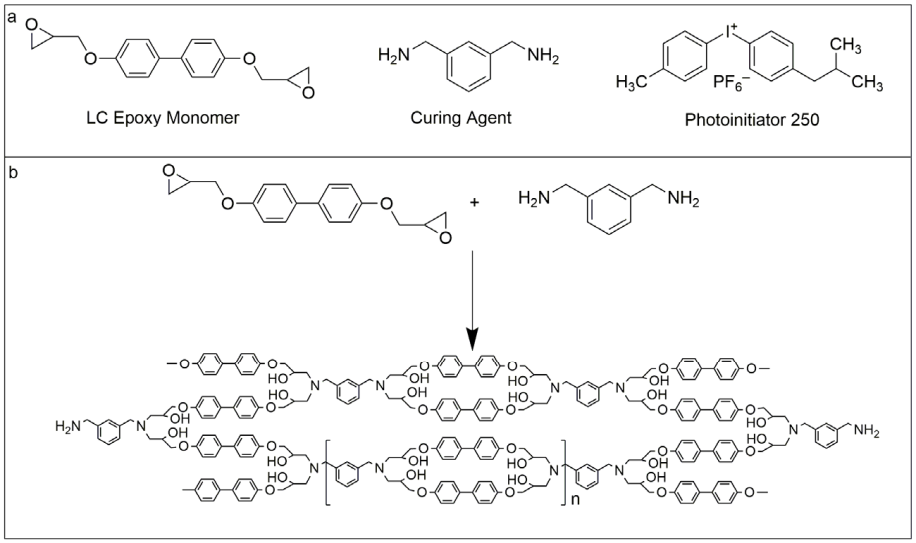

Scheme 1. (**a**) The raw materials for the synthesis of biphenyl epoxy resin (BPEPs), (**b**) The synthetic scheme of BPEPs.

2.3. Characterizations

The thermo-mechanical properties of BPEPs were performed on a dynamic mechanical analyzer (DMA, NETZSCH DMA 242C, Germany) at tensile model, and the temperature program was set as heating from −20 °C to 200 °C with a heating rate of 5 °C min^{-1} and a frequency of 1 Hz. The tested samples were cut into a rectangular shape

($20 \times 3 \times 0.05$ mm^3). The temperature of the maximum peak in loss factor curves can be regarded as glass transition temperature (T_g).

The thermal performance was investigated on a differential scanning calorimetry (DSC, NETZSCH DSC 200F3, Germany). In DSC testing, about 3 mg film sample is used for testing at a nitrogen flow rate of about 20 mL/min. The test temperature ranged from −50 °C to 180 °C, and the heating rate was 5 °C min^{-1}. The glass transition temperature of the sample was determined from the second heating curve.

The mechanical properties were tested by a universal testing machine (Shimadzu, AD-X (5000 N), Tokyo, Japan). The sample was cut into the dog bone shape according to ISO 527-2/1BB, and the tensile speed was set to 5 mm min^{-1}. At least 5 samples were measured to obtain the reliable average value.

The shape memory properties of BPEPs were performed by a dynamic thermomechanical analyzer (DMA, NETZSCH DMA 242C) at tensile mode (TMA). Five circles were measured to evaluate the shape memory effect, and each circle was composed of four steps: deformation, fixation, unloading, and recovery. First, raise the temperature to T_g + 30 °C and stretch the sample under constant force. Second, the temperature was cooled to 20 °C to fix the stress and obtain the temporary shape with the strain ε_{load}. Next, unload the force; the sample with the strain under load-free is defined as ε_{unload}. Finally, raise the temperature to T_g + 30 °C again, and the stretched sample tended to recover load-free; the strain ε_{rec} after recovering at 100 °C for 30 min was obtained. The shape fixation ratio (R_f) and shape recovery ratio (R_r) were calculated according to Equations (1) and (2).

$$R_f = \frac{\varepsilon_{unload}}{\varepsilon_{load}} \times 100\% \quad (1)$$

$$R_r = \frac{\varepsilon_{unload}(N) - \varepsilon_{rec}(N)}{\varepsilon_{unload}(N) - \varepsilon_{rec}(N-1)} \times 100\% \quad (2)$$

The tribological behavior of shape memory biphenyl epoxy resin was carried out on a ball-on-disk tribometer (CSEM-THT07-135, Neuchatel, Switzerland) at a different temperature; the schematic tribometer is shown in Figure 1. First, the prepared film was cut into a circle with a diameter of 25.4 mm and pasted onto a cylinder with a diameter of 25.4 mm and a height of 6 mm using polyimide Kapton. The film thickness on the surface of the cylinder is about 0.2 mm, and the GCr15 (AISI 52100) ball (with a diameter of 3 mm) was used as a friction counterpart, whose surface was cleaned with ethanol prior to the test. The speed of 5 cm s^{-1} under a force of 2 N was applied for the test, and the sliding distance was 400 m. The wear volume (V) was measured by a laser confocal three-dimensional profiler (GW-3), then it was applied for the calculation of the wear rate according to the following Equation (3) [30]. In the equation, W refers to the wear rate in unit of mm^3 N^{-1} m^{-1}, V is the wear volume in unit of mm^3, P is the loaded weight in unit of N, and L is the sliding distance in unit of m. The data were collected, and the test was repeated more than 3 times for each sample.

$$W = \frac{V}{PL} \quad (3)$$

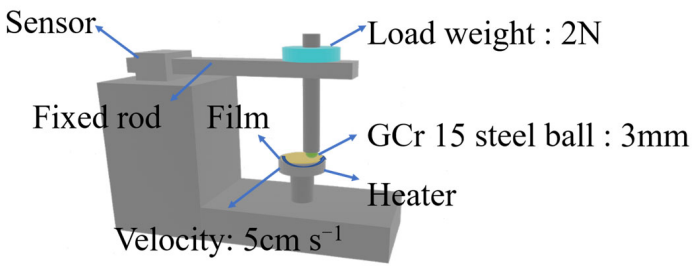

Figure 1. The schematic diagram of the CSM tribometer.

The surface morphology of the GCr15 steel counterpart after the friction test was analyzed by an optical microscope, while the wear trail of the film was investigated by a field emission scanning electron microscope (FESEM, Tescan Mira3, Brno, Czech Republic). Additionally, the elemental composition of the transfer film was analyzed by the energy dispersive spectrometer (EDS) coupled with the SEM. The chemical structure of the BPEPs surface was analyzed by using X-ray photoelectron spectroscopy (XPS, ThermoFisher Scientific, Oxford, UK). A higher resolution X-ray diffractometer (XRD, D8 Discover25) was used to collect both the 1D and 2D XRD patterns of the film sample. The portable thermal conductivity meter (TC3000E, XIATECH) was used to test the thermal diffusion coefficient of the polymer. The Vickers hardness was measured by the MH-5 Vickers indentation method under a normal load of 25 g and resting time of 5 s. At least 5 measurements were made to test the hardness of the samples before and after the friction experiment above the glass transition temperature.

An Angle System OCA 20 (Dataphysics, Filderstadt, Germany) was applied for the contact angles (θ) measurement. The surface energy of BPEPs was calculated by measuring two types of liquid (water, diiodomethane) with different polarity; the calculation formulas are shown as following Equations (4) and (5) [31,32].

$$\gamma_{SV} = \gamma_{SV}^{d} + \gamma_{SV}^{p} \tag{4}$$

$$\gamma_{LV}(1 + \cos\theta_{LV}) = 2\sqrt{(\gamma_{LV}^{d}\gamma_{SV}^{d})} + 2\sqrt{(\gamma_{LV}^{p}\gamma_{SV}^{p})} \tag{5}$$

where γ_{LV} is a surface tension of wetting liquid, γ_{LV}^{d} and γ_{LV}^{p} are dispersive and polar components, respectively. The γ_{SV}^{d} and γ_{SV}^{p} refer to dispersion force and polarity, respectively. The known surface energy of water and diiodomethane was obtained from the software, as listed in Table 1.

Table 1. The surface energy parameters of two kinds of liquid.

Liquid Sample	γ_{LV} (mN/m)	γ_{LV}^{d}(mN/m)	γ_{LV}^{p} (mN/m)
Water	72.8	29.1	43.7
Diiodomethane	50.8	49.5	1.3

3. Results

3.1. Physical and Chemical Properties of BPEPs

The BPEPs with varied crosslinking densities were prepared by adjusting the ratio of epoxy/amine by a photocuring-assisted amine thermal curing, and the characterizations of BPEPs are listed in Table 2. Briefly, the higher ratio of epoxy/amine resulted in the lower crosslinking density (v_e), which varies from 1.2×10^3 mol·m^{-3} to 2.8×10^3 mol·m^{-3} (calculated according to the rubber theory equation [33]) with the epoxy/amine decreased from 1:0.86 to 1:0.5. The storage modulus (E′) at room temperature and 100 °C increase with the increasing of v_e, and the E′ (25 °C, 2.8 GPa) is about 100 times of E′ (100 °C, 25.7 MPa). The elongation at break (ε_b) represents the stretchability that decreases from 43% to 4.5% with the increase in v_e.

Generally speaking, the chemical structure determines the mechanical properties and tribological behaviors of polymers. The aromatic backbone of the BPEPs enables the polymer with high strength, while the rigid biphenyl units provide the switchable property between crystalline and amorphous, and suitable crosslinking density enables the polymer network with sufficient flexibility [34]. Thus, an intriguing tribological behavior was expected to observe. Furthermore, the shape memory polymer is capable of changing shape with the energy conversion in the form of phase transition that may regulate the tribological behavior through changing contact surface morphology or transfer the friction heating [35]. Herein, the detailed friction of shape memory BPEPs with varied crosslinking density was studied.

Table 2. Detailed information on physical and chemical properties of BPEPs [26].

Samples	BPEP1	BPEP2	BPEP3
Epoxy/amine	1:0.5	1:0.68	1:0.86
T_g [1] (°C)	110	101	41
T_g [2] (°C)	83	71	48
E′ (25 °C, GPa)	2.8	2.6	1.6
E′ (100 °C, MPa)	25.7	19.2	11.4
v_e (10^3 mol·m^{-3})	2.8	2.1	1.2
ε_b (%)	4.5 ± 1.4	29.8 ± 11.7	43.0 ± 8.3
σ_b (MPa)	29.9 ± 7.3	25.3 ± 6.6	20.9 ± 4.9
E (MPa)	2043.9 ± 382.1	1772.1 ± 166.5	1389.9 ± 284.3

[1,2] Glass transition temperature (T_g) from DSC and DMA measurement, respectively.

3.2. The Effect of the Molecular Structure on Friction

Since the SMP experienced the phase transition from a glassy state to a rubbery state with the temperature increase across the glass transition temperature, the tribological performance of BPEPs at different temperatures will be varied. Herein, the friction and wear of BPEPs at two typical temperatures: room temperature (RT) and above the glass transition temperature (T_g + 20 °C), which represent the glassy state and rubbery state, were comparably studied. As shown in Figure 2a and Table 3, at room temperature, the frictional coefficient (COF) of BPEPs is quite low within the range of 0.116~0.125, and the wear rate is less than 1.7 × 10^{-5} mm^3 N^{-1} m^{-1}, indicating the self-lubrication and anti-wear of BPEPs. As described in Table 2, the mechanical properties of BPEPs are presented like an elastomer rather than the traditional rigid epoxy resin, which is usually utilized as friction material with high COF due to the high deformation and adhesion caused sliding resistance. The relatively low COF of BPEPs could be ascribed to in terms of special molecular structure. First, the plentiful rigid benzene rings endow it with a high modulus (Scheme 1 and Table 2), which increases the deformation resistance under friction shearing. Second, the layered structure formed by self-assembly of the biphenyl structure due to π–π interaction provides it with strong intramolecular force, which offers a high resistance to be sheared out. In addition, the low surface energy (γ_{SV}) of BPEPs film (Table 4) is comparable to that of silicone resin with low γ_{SV} (<30) [31]. The lower surface energy reflects the lower adhesion force that promotes the reduced friction of BPEP.

Table 3. Detailed information on BPEPs friction at different temperatures.

Temperature	Samples	Coefficient of Friction (COF)	Wear Rate ($\times 10^{-5}$ mm^3 N^{-1} m^{-1})
RT	BPEP1-RT	0.125 ± 0.013	1.27 ± 0.54
	BPEP2-RT	0.120 ± 0.014	1.38 ± 0.26
	BPEP3-RT	0.116 ± 0.007	1.70 ± 0.38
T_g + 20 °C	BPEP1-110 °C	0.175 ± 0.010	6.94 ± 1.95
	BPEP2-90 °C	0.205 ± 0.014	11.34 ± 2.65
	BPEP3-70 °C	0.214 ± 0.010	16.61 ± 1.15

Table 4. The surface energy of the BPEPs films.

Sample	θ (Water)/°	θ (Diiodomethane)/°	γ_{SV} (mN/m)
BPEP1	88.8	60.8	28.46
BPEP2	91.6	66.4	25.29
BPEP3	98.8	60.1	28.85

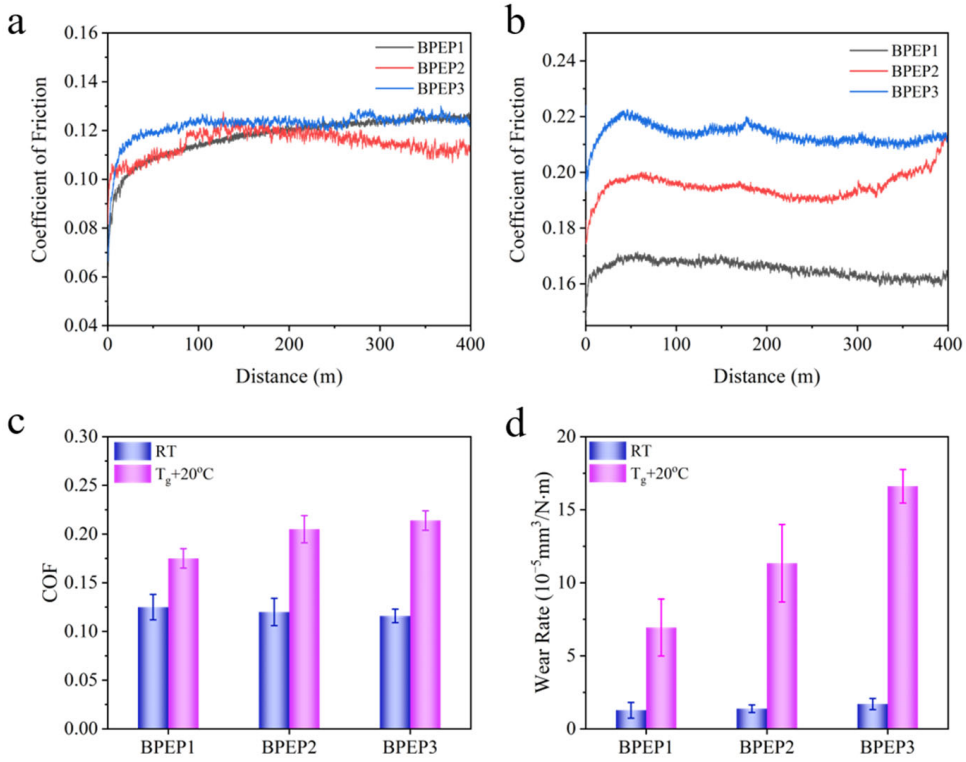

Figure 2. The COF evolution curves of BPEPs at room temperature (**a**) and T_g + 20 °C (**b**), the COF summary (**c**), and the wear rate (**d**) of BPEPs.

When heated the polymer above its T_g, it attains a rubbery state with significantly reduced modulus and increased polymer chain mobility in comparison with that at room temperature; the tribological behavior may perform differently. Usually, under the same load, when the storage modulus is relatively low, the deformation of the material is large and is followed by increased resistance force against the sliding, which results in an increased COF and friction force. For BPEPs, the storage modulus at T_g + 20 °C decreases from 2.8~1.6 GPa to 25.7~11.4 MPa, which is about 100 times lower than that at room temperature; however, the COF increased to 0.175~0.214 (Figure 2b and Table 3). Previously, we found that post-heating of BPEP could facilitate the self-assembly of biphenyl into laminar structure due to π–π interaction; the self-assembly aligned along the direction of friction could counteract the decreased modulus that the COF maintained a relatively low value [26]. Besides the increased COF, the higher molecular mobility at high temperatures allows it to be easier sheared, resulting in the significantly increased wear rate to $(16.61 \pm 1.15) \times 10^{-5}$ mm^{3}N^{-1} m^{-1}.

Reciprocating stretching/contraction during the shape memory cycle induces the self-assembly of the biphenyl that yielded the enhanced mechanical property [36,37], the friction force applied on the BPEP may cause analogous property changes. To explore the effect of friction on BPEP microstructure, the wear scar area after friction test at different temperature were investigated by XRD. Figure 3a,b shows the 1D and 2D XRD patterns of BPEP1 before and after the friction tests at different temperatures. The sharp diffraction peaks at 2θ = 20°, which is attributed to the characteristic diffraction of biphenyl structure, were observed before the friction test [38]. However, two additional diffraction peaks at 22.7° and 28.5° appeared after the RT friction, which is attributed to the lateral stacking between biphenyl units and forming an ordered structure [39,40], indicating the friction-induced crystallization. In comparison, the diffraction peak at 2θ = 20° of the wear scar after the friction test at 110 °C slightly widened, indicating the growth of grain size. Because at a temperature above T_g, the high mobility of the polymer segments allows the mesogens to rearrange and aggregate under the force of friction. Additionally, two diffraction peak appears at 2θ = 31.2°, 47.9° which correspond to the layered structure

formed by biphenyl structure due to the π–π interaction obtained after high-temperature friction. In principle, the microstructure varying could be reflected in the property changing. The Vickers hardness (HV) results (Figure 3c) clearly show the HV increasing from about 16.67 to 23.81 with increase of 43% after the 110 °C friction test. Overall results suggest our reasonable assumption of the achievable friction-induced self-assembly of BPEPs.

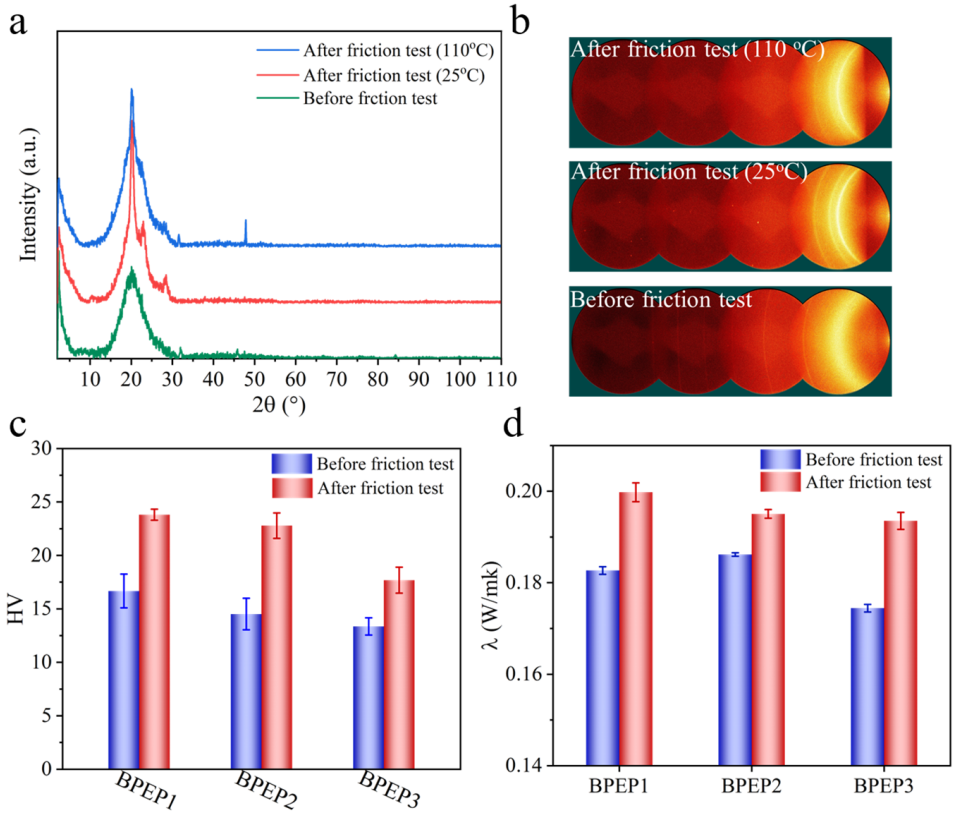

Figure 3. One-dimensional XRD patterns (**a**) and two-dimensional XRD patterns (**b**) of BPEP1 at different states. The Vickers hardness (**c**) and thermal conductivity (**d**) of BPEPs before and after friction test at T_g + 20 °C.

Furthermore, the friction-induced self-assembly of BPEP led to enhanced thermal conductivity, as shown in Figure 3d; the thermal conductivity of BPEP1 after the 110 °C friction test increased from about 0.18 W m^{-1} K^{-1} to 0.2 with an 11% increase. This may attribute to the reduced phonon scattering of harmonic molecular lattice vibrations in the self-assembled structure with higher order [41]. It is significant for the polymer lubrication process, which is beneficial to the friction heat transferring to avoid adhesion wear and tear [42].

3.3. The Effect of the Crosslinking Density on the Friction

Adjusting the content of the curing agent could realize the crosslinking density regulation and physical and chemical properties of polymer tuning. With the increase in curing agent content, the crosslinking density of BPEPs decreased from 2.8 × 10^3 mol·m^{-3} to 1.2 × 10^3 mol·m^{-3}, the tensile strength (29.9~20.9 MPa) and elastic modulus (2~1.4 GPa) of BPEPs are positively correlated with crosslinking density, while the elongation at break (4.5%~43%) is negatively correlated with crosslinking density (Table 2).

The effect of crosslinking density on tribological properties at glassy and rubbery states was comparably tested, and the results are shown in Figure 2 and Table 3. The COF of BPEPs is about 0.116~0.125 at room temperature, and the higher modulus (1.6~2.8 GPa) resulted in no significant difference in COF between different crosslinking densities. However, the effect of crosslinking density on COF at rubbery state is more obvious; the COF increases

from 0.175 to 0.214 with the decrease in crosslinking density from 2.8×10^3 mol·m^{-3} to 1.2×10^3 mol·m^{-3}. At the rubbery state, the crosslinking density plays an important role in the immobilization of the polymer chains, that higher crosslinking density provides higher hardness against the deformation during sliding, therefore decreasing crosslinking density results in the increase in the COF of BPEPs.

As demonstrated in Scheme 1, the high amount of amine added yielded the polymer with a higher amount of free -NH- in comparison with the low amount adding of amine. Figure 4a shows that high content of -NH_2 led to a larger amount of free -NH- in the BPEP polymer network, which is beneficial to the forming of hydrogen bonds. The fine scan XPS spectra of N in BPEPs are shown in Figure 4b; after peak fitting of N1s nuclear grade spectrum, two deconvoluted peaks were observed at 399.9 eV and 401.6 eV, which correspond to C-N and N-H, respectively [43]. With the increase in X-MDA content, the content of N-H in the polymer network increased from 26.96% to 35.37%; as a proton donor, N-H will react with -C=O on the reaction surface of the counterpart to form a weak hydrogen bond. The increased hydrogen bonding is promising to enhance the adhesion with the counterpart that is sheared during the following sliding; this could be the reason for the increase in the BPEP wear rate. Therefore, even though the COF of BPEPs does not change significantly at room temperature, the wear rate shows an increasing trend with the reduction of crosslinking density.

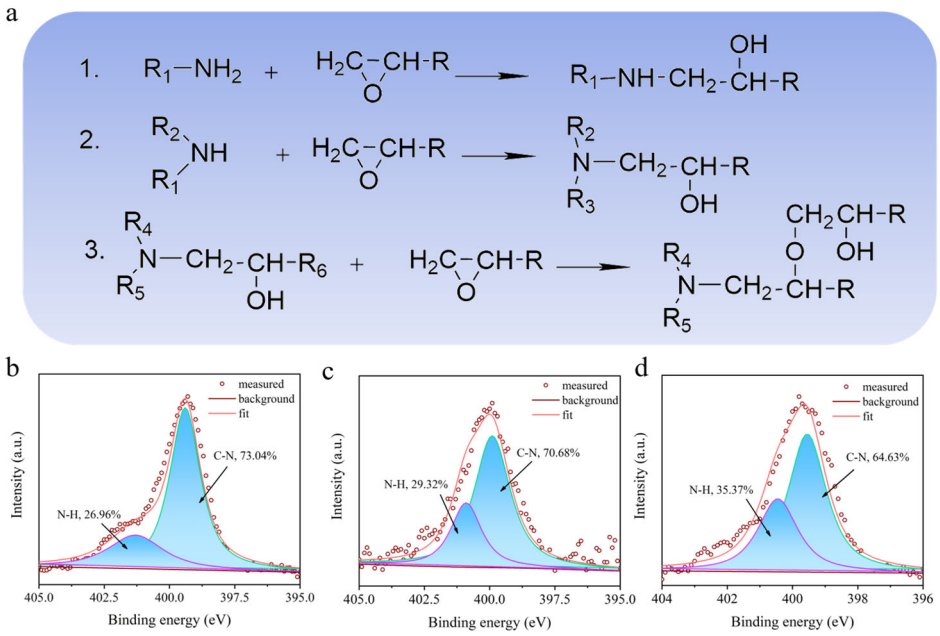

Figure 4. (**a**) Proposed chemical reaction of thermal curing BPEPs. N1s spectra deconvolution in XPS of BPEP1 (**b**), BPEP2 (**c**), and BPEP3 (**d**).

3.4. Thermal Tunable Tribological Behavior

Since the mechanical property of BPEP shows a temperature dependency, the friction and wear properties of BPEP1 at different temperatures were systematically studied. As shown in Figure 5a, the COF of BPEP1 at different temperatures remained stable rapidly after a short period of run-in. The COF of BPEP1 slightly increases from 0.100 ± 0.015 to 0.131 ± 0.012 with the temperature increasing from 25 °C to 70 °C, but it increased significantly to 0.165 ± 0.015 at 90 °C. This change is consistent with the modulus change; with the increase in temperature, the polymer experienced a phase transferring from a glassy state to a high elastic state, and the storage modulus of BPEP1 decreased sharply from 2.8 GPa (25 °C) to 46.2 MPa (90 °C) (Figure 5c). The reduced modulus leads to large deformation during sliding, and the deformation causes a bulge around the counterpart ball, increasing the resistance against the sliding. Thus, the COF increases with the temperature

increasing. When the temperature rises above the glass transition temperature (110 °C), the storage modulus of BPEPs decreases to 12 MPa, which leads to a further increase in the COF to 0.175, which is only 40% higher than that of COF at room temperature (Table 5). Furthermore, the increased wear rate was obtained, and the wear rate increased from 1.27×10^{-5} mm^3 N^{-1} m^{-1} to 6.94×10^{-5} mm^3 N^{-1} m^{-1} with the temperature increasing from 25 °C to 110 °C, as shown in Figure 5b.

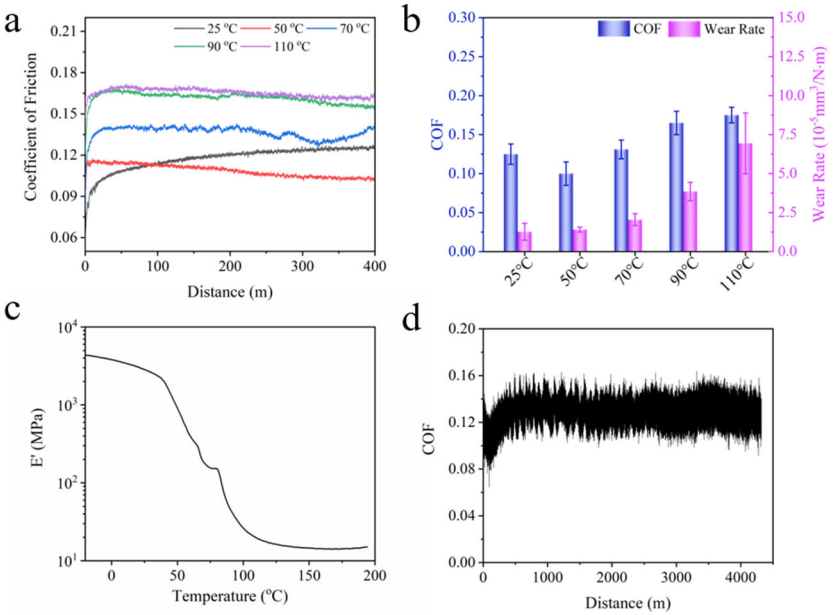

Figure 5. Tribological properties measurement of BPEPs at different temperatures. (**a**) The COF evolution curve of BPEP1 at different temperatures. (**b**) Wear rate and COF summary of BPEP1 at different temperatures. (**c**) The DMA curve of BPEP1. (**d**) The COF evolution curve of BPEP1 with sliding distance (2N, 0.05 m s^{-1}).

Table 5. Detailed information on BPEP1 friction test.

Samples	COF	Wear Rate ($\times 10^{-5}$ mm^3 N^{-1} m^{-1})	E′ (MPa)
BPEP1-25 °C	0.125 ± 0.013	1.27 ± 0.54	2842.4
BPEP1-50 °C	0.100 ± 0.015	1.41 ± 0.16	908.2
BPEP1-70 °C	0.131 ± 0.012	2.01 ± 0.38	183.1
BPEP1-90 °C	0.165 ± 0.015	3.85 ± 0.59	46.2
BPEP1-110 °C	0.175 ± 0.010	6.94 ± 1.95	19.7

As shown in Figure 6b,c, SEM images of wear marks show the width of the wear track increases with the temperature increasing. Compared with the wear marks at room temperature, when the temperature rises to 70 °C, the wear surface becomes rough, so the material wear is more serious. As discussed aforementioned, increasing temperature caused the polymer to transform from a glassy state to a rubbery state, and the storage modulus of BPEP1 decreased gradually (Figure 6a). Thus, the contact area between the polymer substrate and the GCr15 steel counterpart increases gradually, and the width of the wear track increases from 235.29 μm to 299.69 μm with the temperature increasing from room temperature to 70 °C (Figure 6b (I~III)). It is consistent with the optical image of the counterpart ball; Figure 6d (I~III) shows the contact area increases from 0.039 mm^2 to 0.098 mm^2 with the temperature increasing from room temperature to 70 °C. The large wear debris sheets were observed, revealing the typical fatigue wear mechanism; the matrix was peeled by repeated sliding during friction. Moreover, at room temperature, the high modulus of BPEP1 led to a large number of scratches appearing on the surface of the steel

ball. However, the modulus reduction with the temperature rising allows the polymer to be sheared and form the transfer films on the surface of the steel ball (Figure 6d (II~IV)). Nevertheless, when the friction test was applied for BPEP1 at 90 °C, which is close to its T_g, an indistinguishable wear area is shown in Figure 6b (IV); it may be attributed to the shape memory effect (SME) of BPEP1.

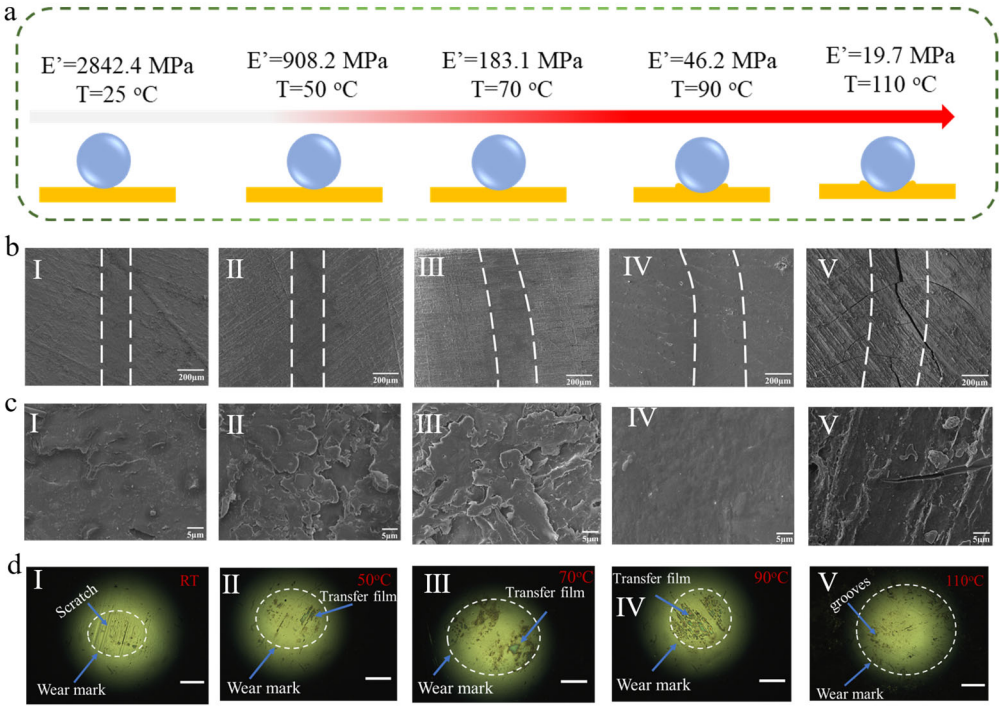

Figure 6. (**a**) Schematic diagram of BPEP1 friction in contact with the counterpart ball at different temperatures. (**b**) The morphology of wear marks after friction tests at different temperatures. (**c**) The corresponding amplified morphology of the wear mark. (**d**) The optical microscope images of the GCr15 steel counterpart after the friction experiments at different temperature, scale bar = 100 μm (I–V are corresponding to the friction test at 25 °C, 50 °C, 70 °C, 90 °C, and 110 °C, respectively).

Due to the inherent shape memory effect of BPEPs (Figure 7a), the temperature can be easily programmed to achieve the transformation between different shapes, which is often accompanied by the transformation of energy (Figure 7b). The shape memory process is schematical demonstrated in Figure 7c,d in terms of macroscopical shape changing and microscopical polymer chain varying, respectively. The relatively higher mobility of polymer chains above the glass transition temperature (T_g) allows it readily rearranged; the π–π stacking of the biphenyl units promotes the polymer chain forming additional physical entanglement to fix the temporary shape. When heat the BPEP above T_g, the maximum conformational entropy drives the molecular chain spontaneously restored to a free state, and the initial shape is obtained [20]. However, the strong π–π stacking remains even after heating, which leads to the gradual enhancement of mechanical properties during the BPEPs shape memory effect cycle. During the high-temperature friction test, the friction counterpart reciprocated sliding on the BPEPs surface; concerning the particular friction area which was periodically bear the contact-leave-contact cycle under a certain load, the deformed surface under the compression tends to shape recovery at a temperature above T_g in the intermittent contact. Furthermore, since the shape memory cycle also involves the transfer of heat energy, the energy conversion from heat to phase transformation is used to drive the shape recovery, so the friction heat of the interface will be consumed as the wear marks tend to recover. Therefore, the shape memory performance of this BPEP realized wear self-compensation (Figure 7e).

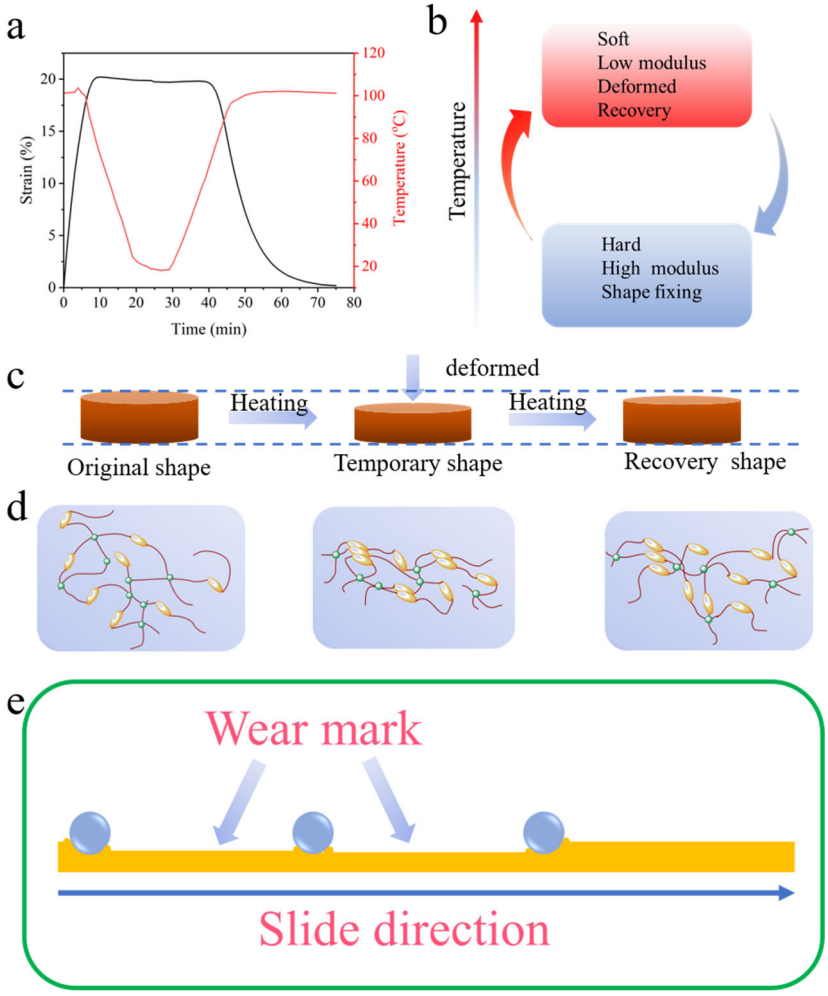

Figure 7. (**a**) The shape memory curve of BPEP1. (**b**) The heat energy transferring in shape memory cycle. Illustration of the shape memory effect of BPEPs with macroscopical shape changing (**c**) and microscopical polymer chain varying (**d**). (**e**) Demonstration of the wear mark surface of the BPEPs in friction test.

Generally, at the transition temperature, the mobility of the polymer chain is higher, the real contact area with the counterpart increases during the friction process, and the elastic deformation is larger. As a result, the sliding resistance, friction coefficient, and wear rate increase significantly, resulting in wear failure. Compared with other polymer materials, BPEP1 still has a lower friction coefficient and wear rate when it transforms from a glassy state to a rubbery state [21,44], which is mainly attributed to the improved mechanical properties of π–π interaction of biphenyl units at high temperature and the self-compensation of wear caused by SME. Nevertheless, when the friction test was conducted at 110 °C, BPEP1 tended to fracture under force due to the chemical bonds breaking at high temperatures. The microcracks along the worn trail were observed (Figure 6b (V)), even though BPEP performed a good self-lubricating with COF = 0.175, which only increased by 40% in comparison with the COF at room temperature. Importantly, this unique temperature responsiveness allows the tribological properties to be regulated.

We explore the long-term self-lubricating reliability of biphenyl epoxy resin. As shown in Figure 6d, after 13.7k cycles of friction test, the COF remains at 0.12 ± 0.01, and the wear rate is $(5.35 \pm 1.77) \times 10^{-6}$ mm^3 N^{-1} m^{-1}. The results indicate the specific anti-friction and wear-resistant of BPEPs with long-term stability and a wide service temperature range. Therefore, BPEP films can be used as a reliable self-lubricating coating material with temperature-tunable tribological performance.

4. Conclusions

In conclusion, the thermal tunable tribological behavior of shape memory biphenyl epoxy resin was systematically studied. The mechanism of friction and wear was discussed by analyzing the microstructure, COF, and wear marks of the surface. The corresponding conclusions are summarized as follows:

1. Due to the special molecular structure with sufficient biphenyl units, BPEPs presented an excellent self-lubricating property in a wide temperature range.
2. Friction induced the self-assembly of the biphenyl unit aligned along the direction of sliding and enhanced the thermal conductivity and hardness that counteract the decreased modulus with temperature increasing; therefore, the COF from 0.175 to 0.214 maintained a relatively low value at a temperature above T_g.
3. The COF and wear rate of BPEP1 friction at T_g + 20 °C increase gradually with the decrease in crosslinking density, which is because the decrease in modulus and the increase in hydrogen bond increase the sliding resistance and adhesion caused by material deformation in the friction.
4. Thermal tunable tribological behavior of BPEPs is based on the mobility varying of the polymer chain and uses the thermal of the friction interface to achieve shape recovery, which is beneficial for reducing friction coefficient and reducing wear.
5. In this study, we first proposed a wear self-compensation mechanism based on shape memory polymer in high-temperature friction experiments, which is conducive to promoting the development of shape memory polymers in the field of tribology. In addition, shape memory polymers can be combined with fillers capable of photothermal conversion, allowing them to achieve intelligent tribological properties by remote control of temperature.

Author Contributions: Conceptualization, J.Y., Q.W. and Y.Z.; Methodology, J.Y., P.C. and Y.Z.; Formal analysis, J.Y., P.C. and K.G.; Data curation, C.D. and K.G.; Writing—original draft preparation, J.Y.; Writing—review and editing, Y.Z. and Q.W.; Project administration, X.Z. and S.C.; Funding acquisition, X.Z., Y.Z., Q.W. and T.W. All authors have read and agreed to the published version of the manuscript.

Funding: This research was funded by the National Key research and development project (2020YFB2006902), National Natural Science Foundation of China (51935012), Major Program of the Lanzhou Institute of Chemical Physics, CAS (No. ZYFZFX-7), CAS Project for Young Scientists In Basic Research (YSBR-023), and Key Research Program of the Chinese Academy of Sciences, Grant NO. XDPB24 (XDPB24).

Institutional Review Board Statement: Not applicable.

Informed Consent Statement: Not applicable.

Data Availability Statement: Not applicable.

Conflicts of Interest: The authors declare no conflict of interest.

References

1. Gong, H.; Yu, C.; Zhang, L.; Xie, G.; Guo, D.; Luo, J. Intelligent lubricating materials: A review. *Compos. Part B-Eng.* **2020**, *202*, 108450. [CrossRef]
2. Huang, X.; Alva, G.; Liu, L.; Fang, G. Microstructure and thermal properties of cetyl alcohol/high density polyethylene composite phase change materials with carbon fiber as shape-stabilized thermal storage materials. *Appl. Energy* **2017**, *200*, 19–27. [CrossRef]
3. Khun, N.W.; Sun, D.W.; Huang, M.X.; Yang, J.L.; Yue, C.Y. Wear resistant epoxy composites with diisocyanate-based self-healing functionality. *Wear* **2014**, *313*, 19–28. [CrossRef]
4. Zhao, H.; Sun, Q.; Deng, X.; Cui, J. Earthworm-Inspired Rough Polymer Coatings with Self-Replenishing Lubrication for Adaptive Friction-Reduction and Antifouling Surfaces. *Adv. Mater.* **2018**, *30*, 1802141. [CrossRef] [PubMed]
5. Ji, Z.; Xie, G.; Xu, W.; Wu, S.; Zhang, L.; Luo, J. Self-Cleaning of Interfacial Oil Between Polymer Composites with Porous Zeolite Microparticles and Their Self-Lubrication Properties. *Adv. Mater. Interfaces* **2019**, *6*, 1801889. [CrossRef]
6. Voevodin, A.A.; Zabinski, J.S. Smart Nanocomposite Coatings with Chameleon Surface Adaptation in Tribological Applications. In *NATO Science Series II: Mathematics, Physics and Chemistry*; Springer: Dordrecht, The Netherlands, 2004.

7. Ren, Y.; Liu, G.; Yang, H.; Tong, T.; Xu, S.; Zhang, L.; Luo, J.; Zhang, C.; Xie, G. Dynamic wear sensor array based on single-electrode triboelectric nanogenerators. *Nano Energy* **2020**, *68*, 104303. [CrossRef]
8. Ruan, H.; Zhang, Y.; Song, F.; Wang, Q.; Wang, C.; Wang, T. Efficacy of hierarchical pore structure in enhancing the tribological and recyclable smart lubrication performance of porous polyimide. *Friction* **2022**. [CrossRef]
9. Ruan, H.; Shao, M.; Zhang, Y.; Wang, Q.; Wang, C.; Wang, T. Supramolecular Oleogel-Impregnated Macroporous Polyimide for High Capacity of Oil Storage and Recyclable Smart Lubrication. *ACS Appl. Mater. Interfaces* **2022**, *14*, 10936–10946. [CrossRef]
10. Shao, M.; Li, S.; Duan, C.; Yang, Z.; Qu, C.; Zhang, Y.; Zhang, D.; Wang, C.; Wang, T.; Wang, Q. Cobweb-like Structural Stimuli-Responsive Composite with Oil Warehouse and Transportation System for Oil Storage and Recyclable Smart-Lubrication. *ACS Appl. Mater. Interfaces* **2018**, *10*, 41699–41706. [CrossRef]
11. Adibnia, V.; Olszewski, M.; De Crescenzo, G.; Matyjaszewski, K.; Banquy, X. Superlubricity of Zwitterionic Bottlebrush Polymers in the Presence of Multivalent Ions. *J. Am. Chem. Soc.* **2020**, *142*, 14843–14847. [CrossRef]
12. Oak, S.; Pashazanusi, L.; Sengel, S.B.; Omarova, M.; Hemstock, J.L.; He, W.; He, J.; John, V.; Sahiner, N.; Pesika, N.S. Tunable Friction Through Stimuli Responsive Hybrid Carbon Microspheres. *Langmuir* **2019**, *35*, 15849–15854. [CrossRef] [PubMed]
13. Liu, G.; Feng, Y.; Zhao, N.; Chen, Z.; Shi, J.; Zhou, F. Polymer-based lubricating materials for functional hydration lubrication. *Chem. Eng. J.* **2022**, *429*, 132324. [CrossRef]
14. Tang, S.; Li, S.; Zhu, S.; Ma, L.; Tian, Y. Light-controlled friction realized by a photorheological fluid. *Tribol. Int.* **2022**, *176*, 107914. [CrossRef]
15. Hua, J.; Björling, M.; Larsson, R.; Shi, Y. Controlling friction in Ionic Liquid/Glycerol Aqueous Solution lubricated contacts by adjusting CO2 and water content. *Tribol. Int.* **2021**, *161*, 107070. [CrossRef]
16. Ma, Y.; Ma, S.; Yang, W.; Yu, B.; Pei, X.; Zhou, F.; Liu, W. Sundew-Inspired Simultaneous Actuation and Adhesion/Friction Control for Reversibly Capturing Objects Underwater. *Adv. Mater. Technol.* **2019**, *4*, 1800467. [CrossRef]
17. Yang, Y.; Pei, Z.; Zhang, X.; Tao, L.; Wei, Y.; Ji, Y. Carbon nanotube–vitrimer composite for facile and efficient photo-welding of epoxy. *Chem. Sci.* **2014**, *5*, 3486–3492. [CrossRef]
18. Xiao, Y.Y.; Jiang, Z.C.; Tong, X.; Zhao, Y. Biomimetic Locomotion of Electrically Powered "Janus" Soft Robots Using a Liquid Crystal Polymer. *Adv. Mater.* **2019**, *31*, 1903452. [CrossRef]
19. Zheng, N.; Fang, G.Q.; Cao, Z.L.; Zhao, Q.; Xie, T. High strain epoxy shape memory polymer. *Polym. Chem.* **2015**, *6*, 3046–3053. [CrossRef]
20. Lendlein, A.; Kelch, S. Shape-Memory Polymers. *Angew. Chem. Int. Ed.* **2002**, *41*, 2034–2057. [CrossRef]
21. Zheng, F.; Bai, Y.; Wang, Q.; Wang, T. Switchable friction properties induced by shape memory effect. *J. Mater. Sci.* **2014**, *49*, 8394–8401. [CrossRef]
22. Liu, D.; Broer, D.J. Self-assembled Dynamic 3D Fingerprints in Liquid-Crystal Coatings Towards Controllable Friction and Adhesion. *Angew. Chem. Int. Ed.* **2014**, *53*, 4542–4546. [CrossRef]
23. Xia, F.; Feng, L.; Wang, S.; Sun, T.; Song, W.; Jiang, W.; Jiang, L. Dual-Responsive Surfaces That Switch between Superhydrophilicity and Superhydrophobicity. *Adv. Mater.* **2006**, *18*, 432–436. [CrossRef]
24. Liu, D.; Broer, D.J. Light controlled friction at a liquid crystal polymer coating with switchable patterning. *Soft Matter* **2014**, *10*, 7952–7958. [CrossRef] [PubMed]
25. Myshkin, N.K.; Kovalev, A. Polymer mechanics and tribology. *Ind. Lubr. Tribol.* **2018**, *70*, 764–772. [CrossRef]
26. Yang, J.; Tao, L.M.; Cao, P.R.; Yang, Z.H.; Zhang, X.R.; Wang, Q.H.; Wang, T.M.; Luo, H.M.; Zhang, Y.M. Biphenyl Containing Shape Memory Epoxy Resin with Post-heating Adjustable Properties. *Macromol. Mater. Eng.* **2021**, *306*, 2100185. [CrossRef]
27. Islam, A.M.; Lim, H.; You, N.-H.; Ahn, S.; Goh, M.; Hahn, J.R.; Yeo, H.; Jang, S.G. Enhanced Thermal Conductivity of Liquid Crystalline Epoxy Resin using Controlled Linear Polymerization. *ACS Macro Lett.* **2018**, *7*, 1180–1185. [CrossRef]
28. Yang, R.; Chen, L.; Ruan, C.; Zhong, H.-Y.; Wang, Y.-Z. Chain folding in main-chain liquid crystalline polyesters: From π–π stacking toward shape memory. *J. Mater. Chem. C* **2014**, *2*, 6155–6164. [CrossRef]
29. Carfagna, C.; Amendola, E.; Giamberini, M.; Hakemi, H.; Pane, S. Liquid crystalline epoxy resins in polymer dispersed liquid crystal composites. *Polym. Int.* **1997**, *44*, 465–473. [CrossRef]
30. Ruan, H.; Zhang, Y.; Li, S.; Yang, L.; Wang, C.; Wang, T.; Wang, Q. Effect of temperature on the friction and wear performance of porous oil-containing polyimide. *Tribol. Int.* **2021**, *157*, 106891. [CrossRef]
31. Zhang, W.; Zou, X.; Liu, X.; Liang, Z.; Ge, Z.; Luo, Y. Preparation and properties of waterborne polyurethane modified by aminoethylaminopropyl polydimethylsiloxane for fluorine-free water repellents. *Prog. Org. Coat.* **2020**, *139*, 105407. [CrossRef]
32. Owens, D.K.; Wendt, R.C. Estimation Of Surface Free Energy Of Polymers. *J. Appl. Polym. Sci.* **1969**, *13*, 1741–1747. [CrossRef]
33. Santiago, D.; Guzman, D.; Ferrando, F.; Serra, A.; De la Flor, S. Bio-Based Epoxy Shape-Memory Thermosets from Triglycidyl Phloroglucinol. *Polymers* **2020**, *12*, 542. [CrossRef] [PubMed]
34. Belmonte, A.; Lama, G.C.; Gentile, G.; Fernandez-Francos, X.; De la Flor, S.; Cerruti, P.; Ambrogi, V. Synthesis and Characterization of Liquid-Crystalline Networks: Toward Autonomous Shape-Memory Actuation. *J. Phys. Chem. C* **2017**, *121*, 22403–22414. [CrossRef]
35. Zhou, J.; Yan, F.; Tian, N.; Zhou, J. Effect of temperature on the tribological and dynamic mechanical properties of liquid crystalline polymer. *Polym. Test.* **2005**, *24*, 270–274. [CrossRef]
36. You, Y.; Huang, X.; Pu, Z.; Jia, K.; Liu, X. Enhanced crystallinity, mechanical and dielectric properties of biphenyl polyarylene ether nitriles by unidirectional hot-stretching. *J. Polym. Res.* **2015**, *22*, 211. [CrossRef]

37. Guo, H.L.; Li, Y.W.; Zheng, J.; Gan, J.Q.; Liang, L.Y.; Wu, K.; Lu, M.G. High thermo-responsive shape memory epoxies based on substituted biphenyl mesogenic with good water resistance. *Rsc Adv.* **2015**, *5*, 67247–67257. [CrossRef]
38. Li, Y.Z.; Pruitt, C.; Rios, O.; Wei, L.Q.; Rock, M.; Keum, J.K.; McDonald, A.G.; Kessler, M.R. Controlled Shape Memory Behavior of a Smectic Main-Chain Liquid Crystalline Elastomer. *Macromolecules* **2015**, *48*, 2864–2874. [CrossRef]
39. Kawamoto, S.; Fujiwara, H.; Nishimura, S. Hydrogen characteristics and ordered structure of mono-mesogen type liquid-crystalline epoxy polymer. *Int. J. Hydrogen Energy* **2016**, *41*, 7500–7510. [CrossRef]
40. Ortiz, C.; Kim, R.; Rodighiero, E.; Ober, C.K.; Kramer, E.J. Deformation of a polydomain, liquid crystalline epoxy-based thermoset. *Macromolecules* **1998**, *31*, 4074–4088. [CrossRef]
41. Choy, C.L. Thermal-Conductivity Of Polymers. *Polymer* **1977**, *18*, 984–1004. [CrossRef]
42. Rasul, G.; Kiziltas, A.; Hoque, S.B.; Banik, A.; Hopkins, P.E.; Tan, K.T.; Arfaei, B.; Shahbazian-Yassar, R. Improvement of the thermal conductivity and tribological properties of polyethylene by incorporating functionalized boron nitride nanosheets. *Tribol. Int.* **2022**, *165*, 107277. [CrossRef]
43. Ahmed, M.H.; Byrne, J.A.; McLaughlin, J.; Ahmed, W. Study of Human Serum Albumin Adsorption and Conformational Change on DLC and Silicon Doped DLC Using XPS and FTIR Spectroscopy. *J. Biomater. Nanobiotechnol.* **2013**, *4*, 194–203. [CrossRef]
44. Wu, Y.Q.; Zeng, M.; Xu, Q.Y.; Hou, S.E.; Jin, H.Y.; Fan, L.R. Effects of glass-to-rubber transition of thermosetting resin matrix on the friction and wear properties of friction materials. *Tribol. Int.* **2012**, *54*, 51–57. [CrossRef]

Disclaimer/Publisher's Note: The statements, opinions and data contained in all publications are solely those of the individual author(s) and contributor(s) and not of MDPI and/or the editor(s). MDPI and/or the editor(s) disclaim responsibility for any injury to people or property resulting from any ideas, methods, instructions or products referred to in the content.